remote sensing

MDPI

Article

Maize Canopy and Leaf Chlorophyll Content Assessment from Leaf Spectral Reflectance: Estimation and Uncertainty Analysis across Growth Stages and Vertical Distribution

Hongye Yang [1,†], Bo Ming [1,†], Chenwei Nie [1], Beibei Xue [1], Jiangfeng Xin [1,2], Xingli Lu [2], Jun Xue [1], Peng Hou [1], Ruizhi Xie [1], Keru Wang [1,*] and Shaokun Li [1]

[1] Key Laboratory of Crop Physiology and Ecology, Institute of Crop Sciences, Chinese Academy of Agricultural Sciences, Beijing 100081, China; 82101195022@caas.cn (H.Y.); mingbo@caas.cn (B.M.); niechenwei@caas.cn (C.N.); 82101205031@caas.cn (B.X.); xinjiangfeng2020@126.com (J.X.); xuejun@caas.cn (J.X.); houpeng@caas.cn (P.H.); xieruizhi@caas.cn (R.X.); lishaokun@caas.cn (S.L.)

[2] School of Agriculture, Ningxia University, Yinchuan 750021, China; xinglilu@nxu.edu.cn

* Correspondence: wangkeru@caas.cn; Tel.: +86-010-82105791

† These authors contributed equally to this work.

Abstract: Accurate estimation of the canopy chlorophyll content (CCC) plays a key role in quantitative remote sensing. Maize (*Zea mays* L.) is a high-stalk crop with a large leaf area and deep canopy. It has a non-uniform vertical distribution of the leaf chlorophyll content (LCC), which limits remote sensing of CCC. Therefore, it is crucial to understand the vertical heterogeneity of LCC and leaf reflectance spectra to improve the accuracy of CCC monitoring. In this study, CCC, LCC, and leaf spectral reflectance were measured during two consecutive field growing seasons under five nitrogen treatments. The vertical LCC profile showed an asymmetric 'bell-shaped' curve structure and was affected by nitrogen application. The leaf reflectance also varied greatly between spatio–temporal conditions, which could indicate the influence of vertical heterogeneity. In the early growth stage, the spectral differences between leaf positions were mainly concentrated in the red-edge (RE) and near-infrared (NIR) regions, whereas differences were concentrated in the visible region during the mid-late filling stage. LCC had a strong linear correlation with vegetation indices (VIs), such as the modified red-edge ratio (mRER, R^2 = 0.87), but the VI–chlorophyll models showed significant inversion errors throughout the growth season, especially at the early vegetative growth stage and the late filling stage (rRMSE values ranged from 36% to 87.4%). The vertical distribution of LCC had a strong correlation with the total chlorophyll in canopy, and sensitive leaf positions were identified with a multiple stepwise regression (MSR) model. The LCC of leaf positions L6 in the vegetative stage (R^2-adj = 0.9) and L11 + L14 in the reproductive stage (R^2-adj = 0.93) could be used to evaluate the canopy chlorophyll status (L12 represents the ear leaf). With a strong relationship between leaf spectral reflectance and LCC, CCC can be estimated directly by leaf spectral reflectance (mRER, rRMSE = 8.97%). Therefore, the spatio–temporal variations of LCC and leaf spectral reflectance were analyzed, and a higher accuracy CCC estimation approach that can avoid the effects of the leaf area was proposed.

Keywords: leaf chlorophyll content; canopy chlorophyll content; vertical distribution; leaf spectral reflectance; maize

Citation: Yang, H.; Ming, B.; Nie, C.; Xue, B.; Xin, J.; Lu, X.; Xue, J.; Hou, P.; Xie, R.; Wang, K.; et al. Maize Canopy and Leaf Chlorophyll Content Assessment from Leaf Spectral Reflectance: Estimation and Uncertainty Analysis across Growth Stages and Vertical Distribution. *Remote Sens.* **2022**, *14*, 2115. https://doi.org/10.3390/rs14092115

Academic Editor: Yingying Dong

Received: 23 February 2022
Accepted: 26 April 2022
Published: 28 April 2022

1. Introduction

The canopy chlorophyll content (CCC) can reflect the total photosynthetic productivity of a population, and it forms an important basis for judging the growth and nutritional status of individual plants [1–3]. Accurate monitoring of the chlorophyll content at the canopy and leaf scales by remote sensing is key in crop growth status determination and yield prediction [2,4]. However, the chlorophyll content in the maize canopy has a strong

non-uniform vertical distribution, which makes it difficult to monitor CCC by standard spectral methods [5,6].

The non-uniform vertical profile of CCC in the canopy is generally abstracted as a slightly skewed "bell-shaped" model or Gaussian curve structure [7,8], with higher levels in the middle and lower levels at the top and bottom of the canopy. This means that the leaf chlorophyll content (LCC) at each leaf position is different. Light and nitrogen availability are the main factors that affect the vertical distribution of LCC in the canopy [7,9,10]. Transference and reuse of nitrogen between leaf layers during the growth season amplifies the spatio–temporal variability of LCC in the canopy [5,11]. Therefore, comprehensive measurements of the temporal and spatial distribution of chlorophyll in the canopy are required for accurate evaluation of the growth and nutritional status of maize in the field.

Vegetation indices (VIs) based on visible and near infrared (NIR) regions are well correlated with LCC, and the sensitive wavebands are primarily between 520 and 585 nm and 695 and 740 nm [12–14]. The empirical VI method, which is based on combinations of wavebands, can be used for accurate quantitative remote sensing of the chlorophyll content; this has been demonstrated in numerous studies. Common and widely used VIs include the normalized difference red edge index (NDRE) [15], MERIS Terrestrial Chlorophyll Index (MTCI) [16], and Vogelman Red Edge Index 2 (VOG2) [17]. In particular, the red edge chlorophyll index ($CI_{red\text{-}edge}$) has been found to have a strong correlation with LCC ($R^2 > 0.94$) [18] and can be used to accurately estimate LCC within a range of 10–80 $\mu g/cm^2$ [8,18]. Based on the spectral reflectance, VI has strong adaptability and expansibility, and previous studies developed diverse VI models to reduce the influence of factors such as the leaf structure, surface reflectance, and soil background on chlorophyll inversion accuracy [4,13,19]. Other studies developed transferable leaf nitrogen content assessment models based on support vector regression (SVR) and partial least squares regression (PLSR) to account for variations in plant species and growth conditions [20,21]. Physically based radiation transfer models (RTM) such as PROSPECT and PROSAIL have been widely used to simulate leaf hyperspectral reflectance and to optimize chlorophyll inversion methods at the leaf and canopy scales [22–24].

Although the methods described above function well in some applications, the vertical heterogeneity of LCC in the canopy and between growth stages causes significant differences in reflectance spectrum characteristics of leaves in different positions [14,25]. Soil and Plant Analyzer Development (SPAD-502) is a widely used chlorophyll meter, and it has been demonstrated that the relationship between SPAD values and LCC is not consistent between different leaf positions [26,27]. The high-value area of SPAD generally appears in the middle–upper rank of leaves and changes with nitrogen supply [7]. The correlation between leaf reflectance and the chlorophyll content has been shown to be highest in the middle–upper positions [14,27], and LCC-based inversion accuracy of VI is higher in the middle than in upper or lower positions. In studies of canopy vertical distribution, the canopy is often artificially divided into upper, middle, and lower layers, and corresponding spectral index models have been established based on that system [27–29]. There has been no clear conclusion regarding how the relationships between leaf spectral characteristics and LCC change in different growth stages and leaf positions in the canopy.

CCC is a comprehensive evaluation of the chlorophyll content at the canopy scale; estimation of CCC is affected by the vertical distribution of LCC [5,30]. The vertical distribution of LCC in the canopy can be adjusted to increase the photosynthetic rate of leaves in the upper canopy to cope with stress conditions [31]. Symptoms of chlorophyll deficiency often occur in the lower layers, and the mid-upper layers show significant changes in LCC when nitrogen supply is altered [14,28,31]. The collar leaf and the ear leaf have generally been used before and after silking, respectively, as the "sensitive leaf" to estimate the canopy chlorophyll status [30,32]. Previous studies demonstrated a strong relationship between chlorophyll accumulation in the ear leaf and CCC ($R^2 = 0.86$) [30]. It has also been suggested that the mean LCC of upper canopy layers can be used to represent all canopy layers, and therefore CCC can be estimated as the mean $LCC_{upper} \times$ leaf area

index (LAI) (R^2 = 0.97) [33]. Estimation of CCC based on canopy spectral reflectance is an efficient and convenient method but seldom takes non-uniform chlorophyll distribution into consideration [34,35]. This limits the accuracy of CCC remote sensing (R^2 = 0.60) and decreases the practical value [35]. Due to the vertical variability of LCC between growth conditions, it is not known whether CCC can be accurately evaluated by LCC. If it can, LCC measurements could be used as a quick method to determine the canopy chlorophyll status.

In this study, we used a gradient of five nitrogen treatments to establish a range of canopy architectures, sampled all of the leaves in the canopy throughout the growth season, and measured LCC and leaf spectral reflectance. Three objectives were addressed: (1) to understand the effect of nitrogen supply on the vertical distribution of chlorophyll in the maize canopy and dynamic changes in chlorophyll distribution during the growth season; (2) to explore differences in leaf spectral reflectance characteristics in the canopy and verify whether a VI model based on leaf spectral reflectance can accurately invert LCC under variable spatio–temporal conditions; and (3) to identify the sensitive leaf positions (those that can be used to characterize the relationship between LCC and CCC) and evaluate the robustness and accuracy of a VI model based on leaf spectra to assess the canopy chlorophyll status.

2. Materials and Methods

2.1. Study Area and Experimental Design

This experiment was conducted in 2019 and 2020 at the Xinxiang Experimental Station (35°7′51.57″N, 113°45′36.63″E) of the Chinese Academy of Agricultural Sciences, Henan Province, Eastern China, located in the Huang-Huai-Hai maize ecological zone. The experimental site was located in a semi-moist monsoon temperate continental climate region, with annual average temperature, precipitation, and sunlight duration of 14 °C, 573.4 mm, and 1993 h, respectively. The maize hybrid 'Jingnongke 728' (JNK728) was used, and the growing season was from 18 June to 29 September 2019 and from 11 June to 28 September 2020. The planting density was 75,000 plants/ha, and an isometric planting mode was used. The experimental area was ~0.66 hm^2 with a long-term rotation between summer maize (*Zea mays* L.) and winter wheat (*Triticum aestivum* L.). The soil composition was measured prior to nitrogen fertilizer application; organic matter content was 17.78 g/kg, available P was 12.93 mg/kg, available K was 139.09 mg/kg, total N was 1.34 g/kg, and the pH was 7.6.

The experiment in 2019 was a trial, which was followed by the formal experiment in 2020. To obtain a wide range of LCC values and a variety of canopy structures, the experiment was designed with five nitrogen application rate (N rate) treatments: 0, 100, 200, 300, and 400 kg/hm^2 (denoted as N0–N400). The same nitrogen treatment plants and field management practices were followed in 2019 and 2020. In 2019, only the N0 and N400 plants were sampled, whereas plants from all five N treatments were sampled in 2020. Nitrogen fertilizer was applied at the three-leaf (V3) and silking (VT) stages for a total of two applications. Details about the volume and timing of N treatments are shown in Table 1.

Table 1. Nitrogen treatments (kg/hm^2).

Stage	N0	N100	N200	N300	N400
V3	0	60	120	180	240
VT	0	40	80	120	160

A drip irrigation system was used in this study with water and nitrogen fertilizer integrated. Each plot was equipped with a flow gauge to ensure uniform irrigation. Each N treatment had three independent replicate plots, each 9.6 m × 9.6 m (92.16 m^2) in size. The N treatment consisted of urea with a nitrogen content of 46%. Superphosphate was used as phosphate fertilizer (P_2O_5, 12%, 90 kg/hm^2), and potassium chloride was used as potash fertilizer (K_2O, 60%, 120 kg/hm^2), both of which were applied once as basal

fertilizer before sowing. The layout and management of the experimental site were shown in Figure 1.

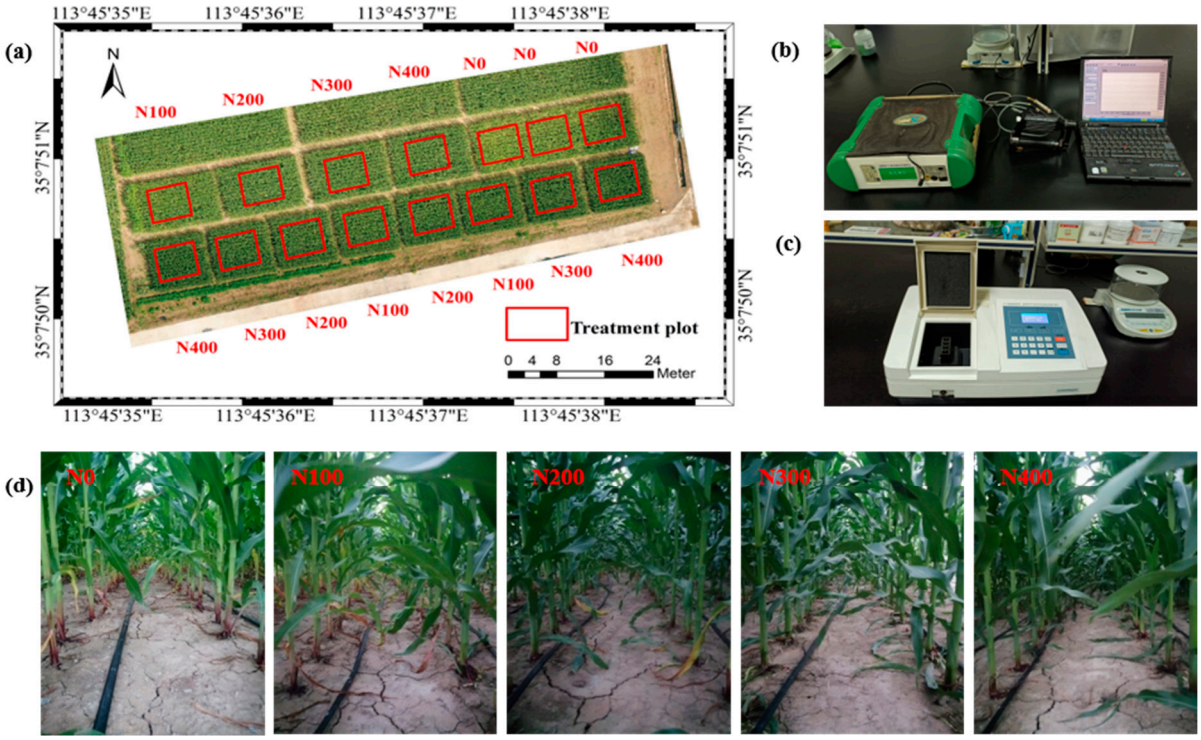

Figure 1. Overhead view of the study area on 2 September 2020 (**a**). Hyperspectral reflectance measurement system (**b**). Benchtop chlorophyll spectrophotometer (**c**). Canopy conditions under five nitrogen treatments (N) on 8 August 2020 (**d**).

2.2. Leaf Sampling and Chlorophyll Measurement

In 2019, samples were collected at three stages during the maize growing season: the sixteen-leaf stage (day 51 after emergence), silking stage (day 64), and filling stage (day 87). In 2020, samples were taken at five stages: the ninth-leaf stage (day 38), silking stage (day 57), blister stage (day 71), filling stage (day 87), and physiological maturity stage (day 100).

The leaf positions L1–L18 denote leaf order from the bottom to the top of the canopy, with the first leaf after emergence designated L1 and subsequent leaves numbered in order. Three maize plants were measured in each plot. For each plot, leaves at the same position were measured as biological replicates of LCC and leaf spectral reflectance. Leaf height was measured as the vertical distance from the leaf collar to the ground. Chlorophyll and spectral reflectance measurements were carried out in the laboratory using ~3800 destructively sampled leaves.

LCC ($\mu g/cm^2$) was measured under dark conditions in the laboratory. A circular punch (10 mm in diameter) was used to obtain leaf discs from symmetrical positions on both sides of the leaf vein. LCC was measured in the basal, central, and top portions of each leaf. Approximately 20 leaf discs were obtained for each leaf position, from which six discs were randomly selected, placed in a test tube, soaked in 95% ethanol (10 mL), and incubated in the dark for 48 h until the chlorophyll was completely extracted. The absorbance values of the chlorophyll solution were measured at 645 and 663 nm using a V-1800BPC spectrophotometer (V-1800, Inc., MAPADA, Shanghai, China), with 95% ethanol as the blank sample. The Arnon method was used to calculate the chlorophyll content [36]:

$$Chl_{a+b}(\mathrm{mg/L}) = 8.04 \times A_{663} + 20.29 \times A_{645} \quad (1)$$

$$LCC\left(\mu g/cm^2\right) = \frac{Chl_{a+b}(mg/L) \times V_T(mL)}{disc\ area(cm^2)} \quad (2)$$

where A_{663} and A_{645} represent the absorbance values of the chlorophyll solution at 663 nm and 645 nm, respectively; V_T (mL) represents the volume of the chlorophyll soaking solution; and *disc area* $\left(cm^2\right)$ represents the area of the leaf disc.

The canopy chlorophyll content (*CCC*, g/m^2) was used to represent the chlorophyll status of the canopy. *CCC* was calculated as the total chlorophyll accumulation per unit of ground area. The leaf area at each leaf position was calculated by manually measuring the maximum *length* and *width* of the leaf [37]:

$$Leaf\ area\left(cm^2\right) = \begin{cases} length \times width \times 0.5\ (Unexpanded\ leaf) \\ length \times width \times 0.75\ (expanded\ leaf) \end{cases} \quad (3)$$

$$CCC\left(g/m^2\right) = \sum_{i=1}^{n}(LCC_i \times LAI_i) \times 100 \quad (4)$$

where n represents the number of leaves in the canopy; LCC_i and LAI_i represent the leaf chlorophyll content ($\mu g/cm^2$) and leaf area index (m^2/m^2) of each leaf position, respectively.

2.3. Leaf Spectral Reflectance Measurements

Leaf spectral reflectance was measured from 350 nm to 2500 nm using an ASD FieldSpec4 spectrometer (Analytical Spectral Devices, Inc., Boulder, CO, USA) attached via a fiber optic cable to a plant probe (Field of View = 25°) equipped with a leaf clip containing a halogen bulb inside. A white reference panel on the leaf clip was used for reflectance correction. The sampling interval was 1.4 nm from 350 to 1000 nm and 2 nm from 1001 nm to 2500 nm. The hyperspectral data were resampled to 1 nm resolution using a self-driven interpolation method in RS3 6.4.0 (ASD Operation Software, Inc., Spectris, Westborough, MA, USA). The wavelength range between 350 nm to 900 nm was used in this experiment because chlorophyll is most strongly associated with that region [12–14]. To avoid potential errors, reflectance spectra were measured at six points symmetrically distributed over the basal, central, and top portions of the leaf. Each point was scanned 10 times, and the average value was recorded. Standard white reference panel calibration was performed before measurements and once every 10–20 min while measurements were taken.

Measurements at several (three to four) leaf positions were halted during the vegetative period because the leaves grew rolled together at the top of the canopy, which hindered chlorophyll extraction and spectral measurements. Leaf hyperspectral reflectance data were acquired in three stages in 2019 and five stages in 2020 as described above for field sampling.

2.4. Vegetation Index Extraction

LCC has a direct correlation with leaf spectral reflectance. Previous research has resulted in the development of various vegetation indices (VIs). We calculated narrow-band vegetation indices from leaf reflectance spectra [38], and 24 classic chlorophyll-related VIs were used to verify their relationship with LCC (Table 2).

2.5. Statistical Analysis

2.5.1. Construction of the VI–Chlorophyll Model

To ensure a sufficient sample size to fully verify the VI–LCC relationship under various spatio–temporal conditions, 170 of the 824 samples from the 2020 dataset were used in model building to determine the relationship between leaf spectral reflectance and LCC. This dataset contained all possible combinations of leaf positions, nitrogen treatments, and sampling time points. A linear model of VI and LCC was constructed using the least squares method.

Table 2. Vegetation indices (VIs) studied in this experiment.

Vegetation Index (Abbr.)	Formula	Reference
Simple ratio (SR)	Rnir/Rred	[39]
Vogelman Red Edge Index 1 (VOG1)	R740/R720	[17]
Normalized difference vegetation index (NDVI)	(Rnir − Rred)/(Rnir + Rred)	[40]
Normalized difference red edge index (NDRE)	(Rnir − Rre)/(Rnir + Rre)	[15]
Green NDVI (GNDVI)	(Rnir − Rgreen)/(Rnir + Rgreen)	[41]
Plant Pigment ratio (PPR)	(Rgreen − Rblue)/(Rgreen + Rblue)	[42]
Canopy chlorophyll content (CCCI)	NDRE/NDVI	[43]
MERIS Terrestrial Chlorophyll Index (MTCI)	(Rnir − Rre)/(Rre − Rred)	[16]
Vogelman Red Edge Index 2 (VOG2)	(R734 − R747)/(R715 + R726)	[17]
Vogelman Red Edge Index 3 (VOG3)	(R734 − R747)/(R715 + R720)	[17]
Red edge chlorophyll index (CIred-edge)	(Rnir/Rre) − 1	[8]
Green chlorophyll index (CIgreen)	(Rnir/Rgreen) − 1	[12]
Transformed Chl absorption in reflectance index (TCARI)	3[(Rre − Rred) − 0.2(Rre − Rgreen)(Rre/Rred)]	[44]
Structure independent pigment index (SIPI)	(R800 − R445)/(R800 − R680)	[45]
Double difference index (DD)	(R750 − R720) − (R700 − R670)	[46]
Modified normalized difference (mND705)	(R750 − R705)/(R750 + R705 − 2 × R445)	[13]
Modified simple ratio (mSR705)	(R750 − R445)/(R705 − R445)	[13]
Triangular vegetation index (TVI)	60 × (Rnir − Rgreen) − 100 × (Rred − Rgreen)	[47]
mTVI (red-edge)	60 × (Rnir − Rgreen) − 100 × (Rre − Rgreen)	[47]
Modified chlorophyll absorption ratio index (MCARI)	(Rre − Rred) − 0.2 × (Rre − Rgreen) × (Rre/Rred)	[3]
mNDblue	(Rblue − Rre)/(Rblue + Rnir)	[48]
Double-peak canopy nitrogen index (DCNII)	(R750 − R700)/(R700 − R670)/(R750 − R670 + 0.09)	[49]
Modified red-edge ratio (mRER)	(R759 − 1.8 × R419)/(R742 − 1.8 × R419)	[50]
Enhanced vegetation index (EVI)	2.5 (Rnir − Rred)/(Rnir + 6 Rred − 7.5 Rblue + 1)	[51]

Rblue, Rgreen, Rred, Rre, and Rnir refer to differences in band reflectance. The characteristic bands were designated as follows: 475 nm (Rblue), 560 nm (Rgreen), 668 nm (Rred), 718 nm (Rre), and 842 nm (Rnir).

2.5.2. Model Testing and Verification

Approximately 13 samples for each growth stage and vertical position were used to test the model. The remaining samples (654 from the 2020 dataset and 427 from the completely independent 2019 dataset) were used as a verification set to determine the correlation between chlorophyll and spectral reflectance. The differences in chlorophyll inversion ability of the unified model based on vertical leaf position were verified at the ninth-leaf stage (day 38), silking stage (day 57), blister stage (day 71), filling stage (day 87), and physiological maturity stage (day 100).

2.5.3. Multivariate Regression Model for LCC and CCC

Multivariable stepwise regression (MSR) is a simple and effective method to avoid multicollinearity among factors and to screen characteristic variables [52]. Each new variable was evaluated with an *F*-test, and the existing variables were evaluated with a *t*-test to ensure that all were significant in MSR. Variance inflation factor (VIF) analysis was used to evaluate the collinearity among variables. When VIF > 10, it is generally considered that there is multicollinearity among variables [53]. The MSR model was evaluated with an adjusted coefficient of determination (R^2-adj), which is used to avoid an increase in R^2 caused by the inclusion of a large number of variables in the model. In this study, it was used to determine the sensitive leaf position that can represent CCC and to construct the multiple linear relationship between LCC and CCC. The stepwise algorithm in SPSS v.22 (SPSS Inc., Chicago, IL, USA) was used for leaf layer filtering and model building. MSR was calculated as follows:

$$Y = \alpha_0 + \alpha_1 X_1 + \alpha_2 X_2 + \cdots + \alpha_n X_n + \varepsilon \quad (5)$$

$$R^2 - adj = 1 - \frac{(1 - R^2)(n - 1)}{n - k - 1} \quad (6)$$

where Y is the value of CCC; a_0 is a constant term; X_1, X_2, ... , X_n are the variables; a_1, a_2, ... , a_n are the coefficients; ε represents a random error term; R^2 represents the coefficient of determination; n represents the number of samples; and k is the number of coefficients in the equation. The dataset from 2020 was used to construct the MSR model of LCC and CCC, and the 2019 dataset was used to verify the robustness and accuracy of the model.

2.5.4. Validation Metrics

ViewSpecPro5.7 spectrum processing software was used for leaf spectral data extraction. Python 3.8 was used for data preprocessing and plotting. The coefficient of determination (R^2), root mean square error (RMSE), and relative root mean square error (rRMSE) were used as indices to evaluate the inversion accuracy of the VI model. Pearson's correlation coefficient (r) was used to express the correlation between spectral wavebands and LCC, and p-values were used to evaluate the degree of significance; $p < 0.05$ was considered a statistically significant difference. The statistical equations were as follows:

$$R^2 = 1 - \frac{\sum_{i=1}^{n}(O_i - P_i)^2}{\sum_{i=1}^{n}(O_i - \overline{O}_i)^2} \quad (7)$$

$$\text{RMSE} = \sqrt{\frac{\sum_{i=1}^{n}(O_i - P_i)^2}{n}} \quad (8)$$

$$\text{rRMSE}\ (\%) = \frac{\text{RMSE}}{\overline{O}} \times 100\% \quad (9)$$

where n is the number of samples; O_i is the observed value; P_i is the estimated value from the regression model; and $\overline{O}_i$ is the average observed value. Higher R^2 and lower RMSE and rRMSE values indicate higher accuracy and precision of the model.

3. Results

3.1. Vertical Profile and Temporal Variation of the Leaf Chlorophyll Content

There were drastic differences in the vertical distribution of LCC at different growth periods (Figure 2). In the early growth stage, LCC showed low levels (2.12 to 76.23 μg/cm^2). After the vegetative growth stage, LCC increased rapidly and peaked at the early filling stage, ranging from 37.35 to 97.02 μg/cm^2 (Figure 2a–c). After peaking, LCC slowly decreased until the end of the growing season, at which point it ranged from 1.02 to 59.29 μg/cm^2. The vertical profile of LCC showed a rapid increase from the top to the middle and a slow decrease from the middle to the bottom. During vegetative stages, the vertical profile of LCC increased toward the bottom layer. During the reproductive period, LCC was obviously skewed toward the higher layers (Figure 2a,b). Maximum LCC values were observed in the two to three leaf positions above the ear leaf (Figure 2b,c). The amount of nitrogen applied had a significant effect on LCC in positions throughout the canopy; those with sufficient nitrogen supply maintained high CCC. At the late growth stage, nitrogen-deficient plants showed a rapid decrease in LCC, which was accompanied by chlorosis and senescence in lower leaf positions (Figure 2c–e).

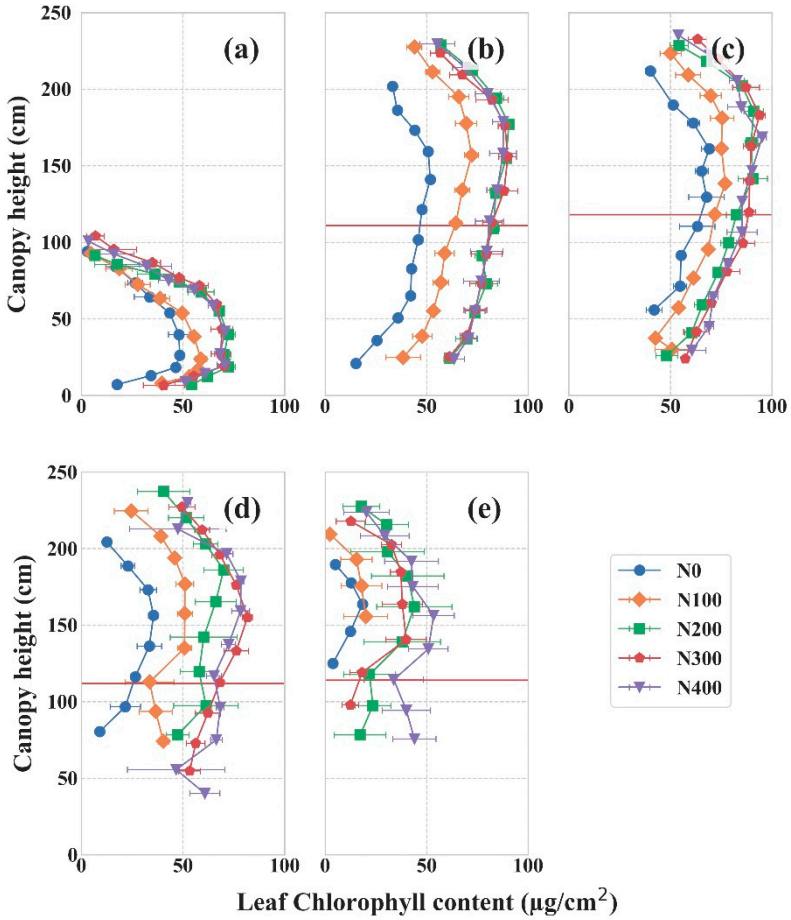

Figure 2. Vertical profile of the leaf chlorophyll content (LCC) within the maize canopy during the 2020 growing season. The y-axis shows the mean height above the ground for each leaf position at five sampling points: (**a**) ninth-leaf stage (day 38), (**b**) silking stage (day 57), (**c**) blister stage (day 71), (**d**) filling stage (day 87), and (**e**) physiological maturity (day 100). The red line denotes the position of the ear leaf (L12). Error bars show standard deviation.

3.2. The Vertical–Temporal Variation of Leaf Reflectance Spectral Characteristics

Samples collected at 38, 57, and 87 days after emergence were used to represent the early (Figure 3a,b), middle (Figure 3c,d), and late (Figure 3e,f) stages of maize growth, respectively. There were significant differences in leaf spectral reflectance curves under different temporal and spatial conditions. In the early growth stage, the main variations in leaf spectral reflectance curves were concentrated in the near-infrared (NIR) band (around 750–900 nm) and the red-edge (RE) band (around 700–721 nm), whereas differences were mostly concentrated in the visible wave band (around 510–680 nm) in the late growth stage. In the middle growth stage, the leaf spectral reflectance curves at different leaf positions were relatively uniform. These obvious fluctuations in reflectance spectra between leaf positions reflect a vertical non-uniformity of leaf properties in the maize canopy.

Leaf position was shown to influence the leaf spectral reflectance. Based on the correlation between wavebands and LCC at different leaf positions, the characteristic of LCC wavebands showed changes in sensitivity at different leaf positions (Figure 3). With the increase in LCC, the RE position moved in the infrared direction, the reflectance spectra in the visible light area showed a descending trend, and the NIR area showed an ascending trend. The sensitive wavebands for LCC were concentrated in the green band (531–567 nm; $r = -0.65$) and the RE band (712–731 nm; $r = -0.77$). There was a weak positive correlation between the NIR band and LCC.

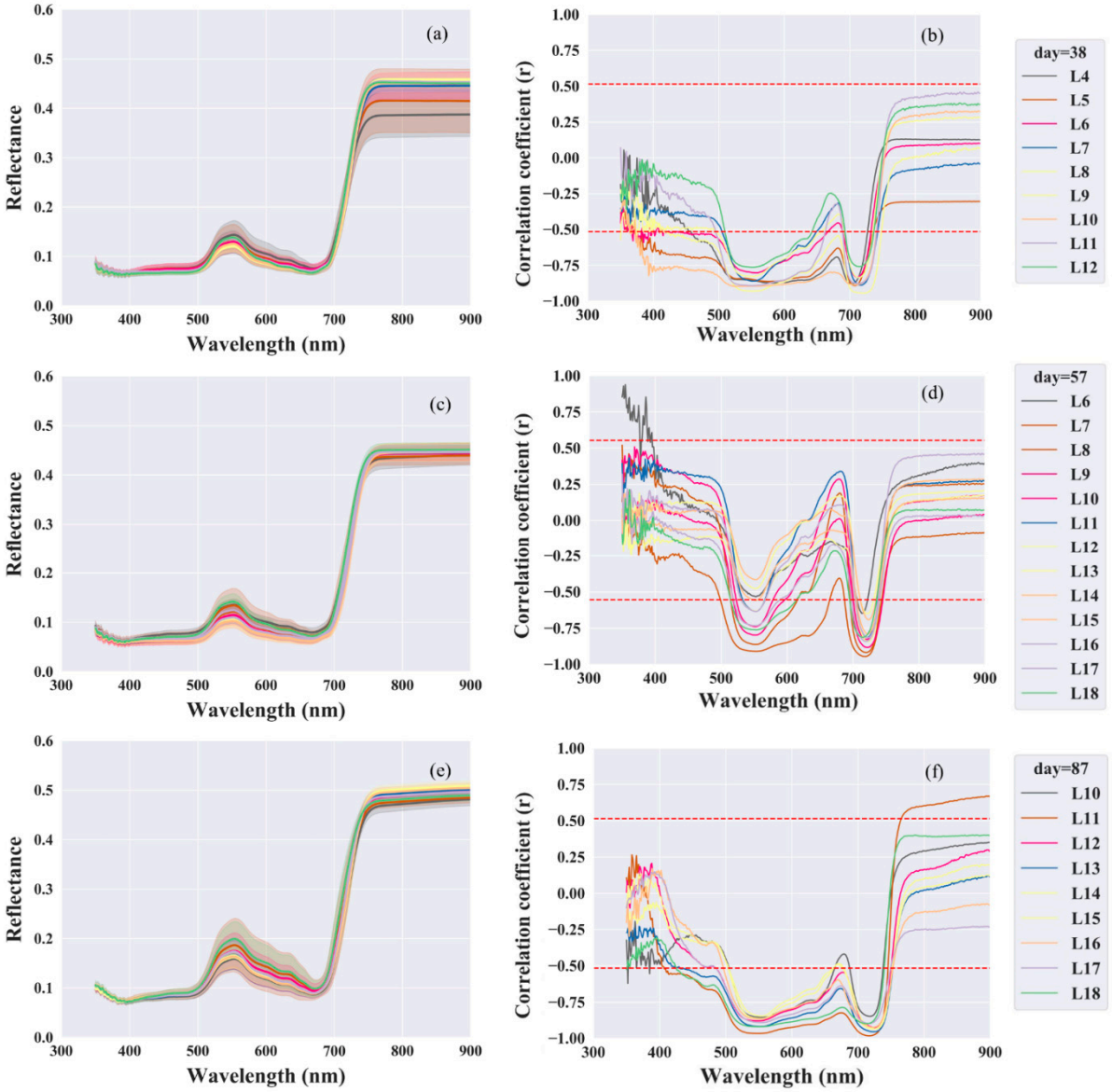

Figure 3. (**a**,**c**,**e**) Spectral reflectance curves for leaves at different positions. The standard deviation interval is shaded in gray. (**b**,**d**,**f**) Correlation coefficient curve for wavebands and the leaf chlorophyll content (LCC) at different leaf positions. The red dashed line indicates $p = 0.05$. L1–L18 indicate leaf positions from the bottom to the top of the canopy. Chlorophyll-related reflectance in the range of 350 to 900 nm was used.

3.3. Sensitivity of Vegetation Indices

Linear models were established to represent the relationship between vegetation indices (VIs) and LCC using the modeling dataset. After models were built, VI sensitivity to LCC was analyzed by calculating the coefficient of determination (R^2), root mean square error (RMSE), and relative RMSE (rRMSE) (Table 3).

The results showed that several commonly used VIs, such as the normalized difference red edge (NDRE), simple ratio (SR), and $CI_{red\text{-}edge}$ had a relatively strong linear correlation with LCC (for example, R^2 for NDRE was 0.85). These VIs are calculated with a combination of near-infrared (NIR) and red-edge band (RE) data, indicating that those two bands had a good inversion ability for LCC under relatively complex conditions. In contrast, green NDVI (GNDVI, NIR and green band; $R^2 = 0.77$) and the normalized difference vegetation

index (NDVI, NIR and red band; R^2 = 0.41) did not perform as well. These results indicate that the red edge band was key for monitoring LCC through the spectral reflectance.

Table 3. Verification of vegetation index (VI) sensitivity to leaf chlorophyll content (LCC).

NO.	VI	Linear Model	R^2	RMSE	rRMSE (%)
1	mRER	y = 496.61x − 499.81	0.87	7.98	14.42
2	VOG2	y = −441.07x + 6.09	0.85	8.38	15.13
3	SR(Rnir, Rre)	y = 65.38x − 66.96	0.85	8.49	15.34
4	CIred-edge	y = 65.38x − 1.58	0.85	8.49	15.34
5	VOG3	y = −377.01x + 8.38	0.85	8.58	15.49
6	NDRE	y = 250.7x − 18.53	0.85	8.59	15.51
7	mTVI	y = 5.85x + 9.47	0.82	9.21	16.64
8	VOG1	y = 103.37x − 104.75	0.82	9.31	16.82
9	MTCI	y = 43.88x − 1.33	0.81	9.48	17.12
10	DD	y = 316.21x + 11.8	0.81	9.50	17.16
11	mNDblue	y = 321.09x + 161.16	0.80	9.93	17.94
12	mSR705	y = 11.44x − 1.51	0.79	10.03	18.11
13	CIgreen	y = 27.06x − 11.9	0.78	10.30	18.61
14	CI705	y = 28.17x − 0.47	0.78	10.40	18.79
15	GNDVI	y = 236.7x − 72.78	0.77	10.50	18.96
16	CCCI	y = 222.07x − 37.6	0.75	10.96	19.80
17	DCNII1	y = 20.16x + 0.38	0.74	11.27	20.36
18	TCARI	y = −201.47x + 115.49	0.49	15.72	28.38
19	MCARI	y = −604.4x + 115.49	0.49	15.72	28.38
20	PPR	y = −245.18x + 125.12	0.42	16.75	30.25
21	NDVI	y = 150.7x − 49.53	0.41	16.89	30.50
22	EVI	y = 131.18x − 34.95	0.27	18.77	33.90
23	SIPI	y = −79.59x + 137.67	0.22	19.43	35.10
24	TVI	y = 1.14x + 26.76	0.02	21.71	39.21

Note: x and y represent VIs and LCC, respectively. A linear model was used to establish the relationship between VI and LCC. *n* = 169.

Some VIs that are composed of three or four wavebands, including multiple red-edge and near-infrared bands, also showed good inversion ability for LCC, such as VOG2 (R^2 = 0.85), mRER (R^2 = 0.87), VOG3 (R^2 = 0.85), MTCI (R^2 = 0.81), and DD (R^2 = 0.81). Previous studies have shown that such VIs have increased robustness and sensitivity compared to dual-band VIs and can reduce the influence of saturation effects [54]. Here, the combination of multiple red-edge bands improved the sensitivity and robustness of the correlation between VIs and LCC.

3.4. Establishing an Inversion Model for Chlorophyll Prediction through Vegetation Indices

To comprehensively verify the accuracy of VI–LCC models throughout the whole growth period, six typical vegetation indices (mRER, VOG2, $CI_{red\text{-}edge}$, NDRE, MTCI, and DD) with different formula types and waveband compositions were selected based on R^2 and RMSE values (Table 3). All six VI models constructed had strong linear (or close to linear) relationships with LCC (Figure 4), with the exception of DD, which showed a slight tendency toward exponential function distribution. The model dataset showed a normal distribution (Figure 4), which met the requirements for random sampling and could therefore be used to represent the whole dataset. However, mRER (Figure 4a), $CI_{red\text{-}edge}$ (Figure 4c), and MTCI (Figure 4e) showed a more uniform data distribution, whereas NDRE (Figure 4d) and DD (Figure 4f) showed a slight skewness toward high values, indicating that there was some saturation at higher LCC values. VOG2 (Figure 4b) was the only VI among the six selected that was negatively correlated with LCC.

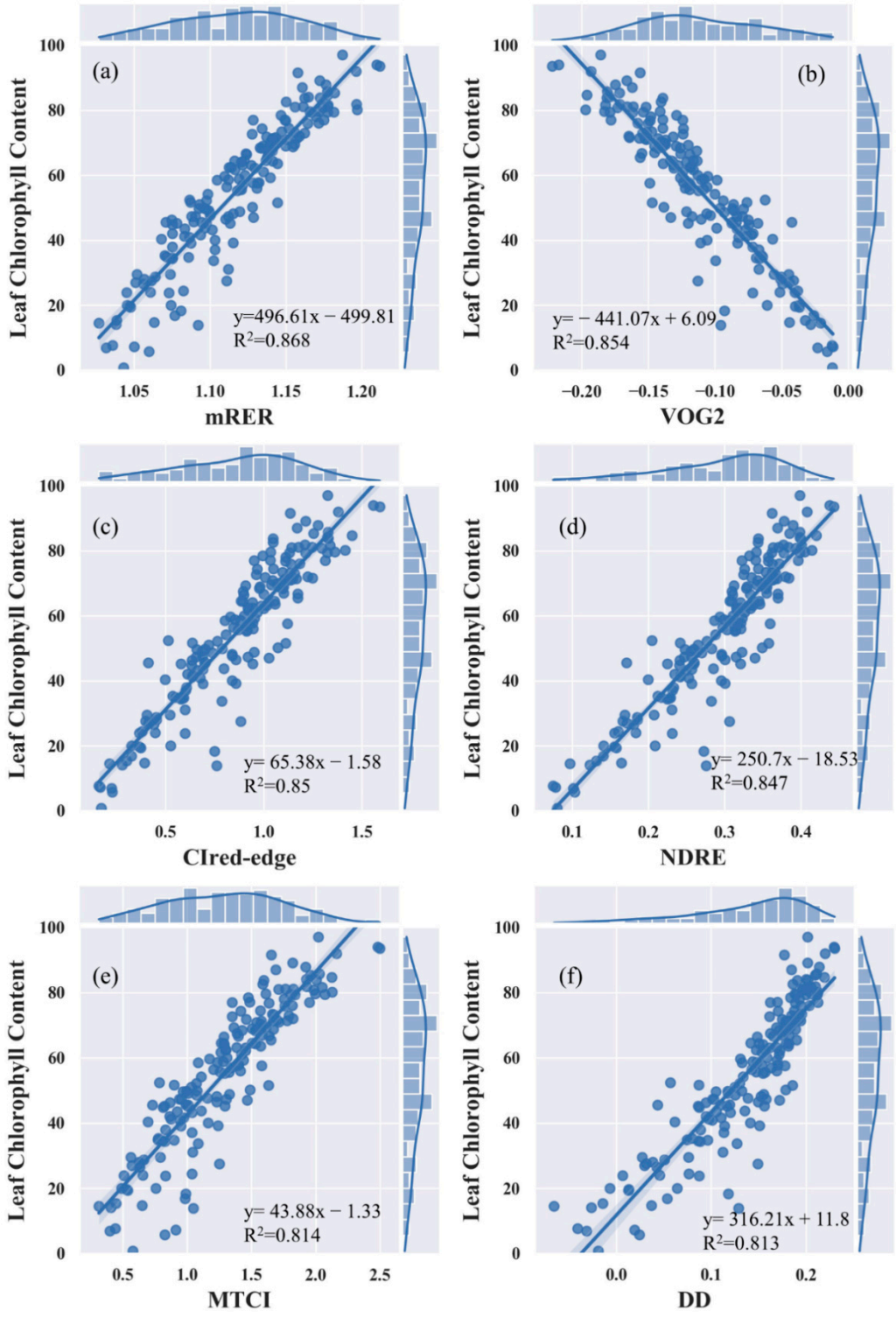

Figure 4. Relationship between LCC and six selected vegetation indices (VIs): (**a**) modified red-edge ratio (mRER), (**b**) Vogelman red edge index 2 (VOG2), (**c**) red edge chlorophyll index ($CI_{red\text{-}edge}$), (**d**) normalized difference red edge index (NDRE), (**e**) MERIS terrestrial chlorophyll index (MTCI), and (**f**) double difference index (DD). Linear models were built using the 2020 modeling dataset. Correlation coefficients and *p*-values are shown above each scatterplot, and the distributions of VI and LCC values are shown as histograms at the top and side of each graph, respectively.

3.5. Validation and Testing under Spatio–Temporal Variation

To verify the relationship between leaf spectral reflectance and the vertical distribution of LCC, VI–chlorophyll models were established to predict LCC under different spatio–temporal conditions (Figure 5). rRMSE was used to express the degree of deviation between the predicted and observed values to measure the robustness and accuracy of each model.

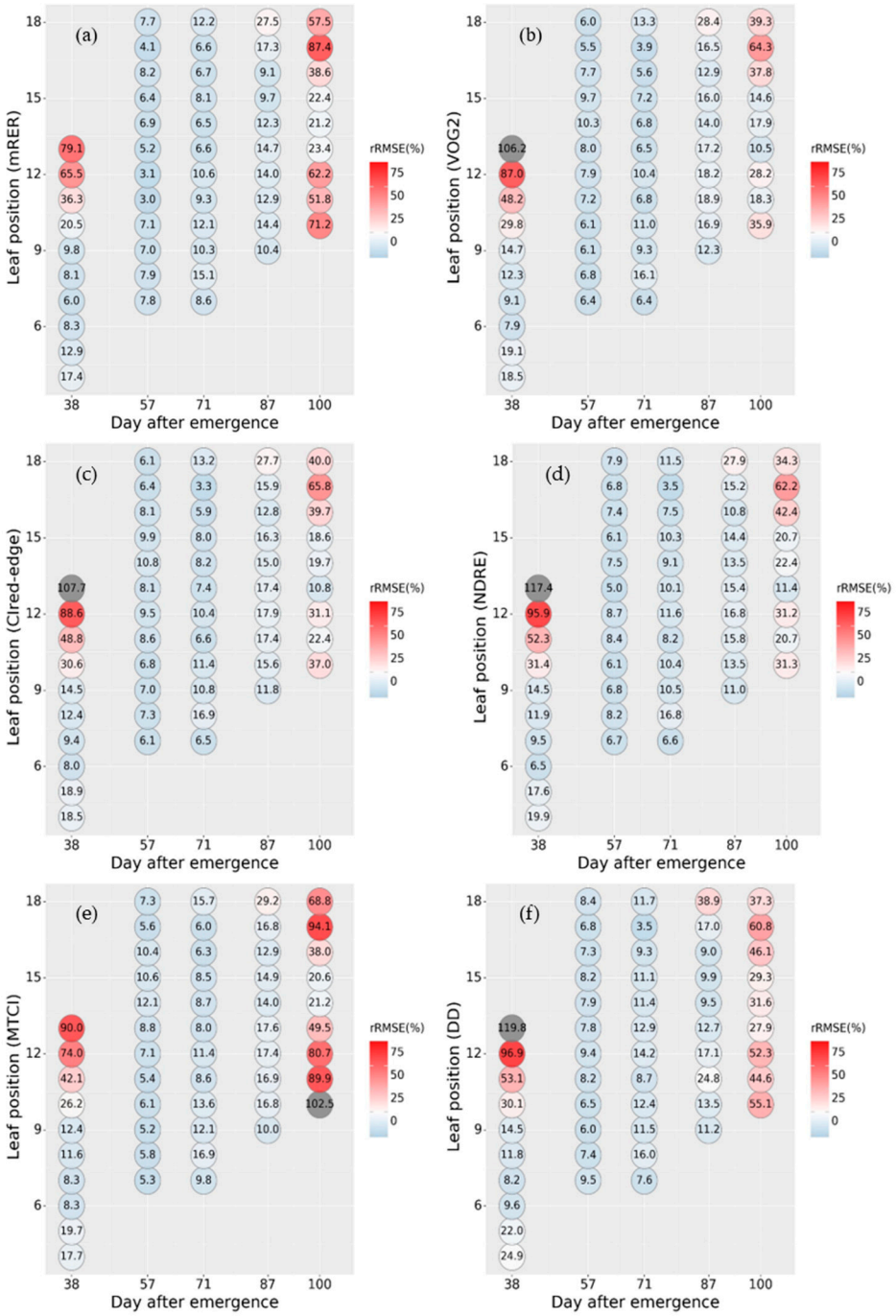

Figure 5. rRMSE (%) for the six LCC-VI models: (**a**) mRER, (**b**) VOG2, (**c**) CIred-edge, (**d**) NDRE, (**e**) MTCI, and (**f**) DD. rRMSE was used to evaluate the model inversion accuracy. Lower values of rRMSE correspond to closer predicted and observed values. The x-axis represents days after first leaf emergence, and the y-axis represents the canopy position where the leaves were located (L1–L18 from the bottom to the top of the plant). Blue indicates a low rRMSE value (low error), and red indicates a high rRMSE value between the observed and predicted LCC. Gray indicates error of more than 100%.

All of the VI models showed a similar pattern in performance throughout the growing season (Figure 5). LCC predictions for the silking stage (day 57) and early filling stage (day 71) had the highest precision, with average rRMSE values of ~6.2% to 9.4%. Precision was lowest in the vegetation stage (day 38) and late growth stage (day 100), with average rRMSE values of ~26.4% to 48.4%. The inversion accuracy of the model also differed by leaf position. In the vegetative growth stage (day 38), the chlorophyll model had a good inversion effect for the lower and middle mature leaves (rRMSE ≈ 10.4%) but not for the top leaf positions with tender leaves (rRMSE ≈ 20% to 80%). In the early and middle reproductive growth stages (days 57, 71, and 87), all leaves in the maize canopy were in a robust mature functional stage, and the chlorophyll model could be used to conduct high-precision inversion for all leaf positions in the canopy (rRMSE ≈ 10.9%). At the end of the growing season when leaves became senescent (day 100), the one to two leaves above the ear leaf (L12), which still had green tissue and maintained basic physiological functions, had the best inversion effect (rRMSE ≈ 21.2%).

In the vegetative growth stage before silking and the late reproductive growth stage, the inversion performance differed significantly by leaf position. This indicated that the relationship between LCC and leaf spectral reflectance was variable, and the inversion accuracy of the VI model was affected by leaf properties or other factors that were vertically distributed in the canopy. A completely independent data set (collected in 2019) was used to test the accuracy of the VI–LCC model. The results are consistent with those shown in Figure 5 (Appendix A/Figure A1). The model had the best inversion precision in the middle growth period (days 51 and 64), and the inversion effect was poor for senescent leaves in the mature stage.

3.6. Relationship between LCC and CCC throughout Growth Stages

Different nitrogen treatments and growth stages were associated with changes in the vertical distribution of chlorophyll in the canopy (Figure 2). There were clear relationships between the chlorophyll content in individual leaves (LCC, $\mu g/cm^2$) located at different leaf positions and the total chlorophyll content in the canopy (CCC, g/m^2), and these relationships varied between growth stages (Figure A2). A multiple stepwise regression model (MSR) was used to determine the sensitive leaf position and to construct a multiple linear relationship between LCC and CCC using the 2020 dataset (Table 4). Variance inflation factor (VIF) analysis was used to measure the degree of collinearity among variables. Variables are generally considered to have multicollinearity when VIF > 10. It is important to note that, due to the correlation between LCC and vertical leaf position, the multivariate linear model for LCC and CCC could incorporate data from a maximum of two leaf positions.

Table 4. Relationships between the leaf chlorophyll content (LCC) and canopy chlorophyll content (CCC) in the 2020 dataset.

MSR Model	Parameters	Regression Model	R^2-adj	Beta	VIF
Early model (day 38)	X_1:L6	$Y = 0.042X_1 - 1.6$	0.9	0.95	1
Middle model (day = 57 + 71)	X_1:L9	$Y = 0.052X_1 - 0.334$	0.89	0.95	1
	X_1:L9, X_2:L16	$Y = 0.038X_1 + 0.018X_2 - 0.79$	0.93	(0.7, 0.3)	2.64
Late model (day = 87 + 100)	X_1:L14	$Y = 0.039X_1 - 0.67$	0.92	0.96	1
	X_1:L14, X_2:L9	$Y = 0.032X_1 + 0.009X_2 - 0.362$	0.97	(0.79, 0.27)	1.74
Reproductive model (day 57−100)	X_1:L11	$Y = 0.042X_1 - 0.09$	0.91	0.95	1
	X_1:L11, X_2:L14	$Y = 0.022X_1 + 0.024X_2 - 0.679$	0.93	(0.51, 0.48)	8.428

Notes: Using the 2020 data, the samples were divided into early, middle, late, and reproductive stages based on the number of days after emergence. CCC (g/m^2) was the dependent variable, and LCC ($\mu g/cm^2$) was the independent variable. X_1 and X_2 represent the sensitive leaf positions determined by MSR. Beta represents the contribution of different parameters to the model, and VIF represents the degree of collinearity between parameters. VIF > 10 indicates strong collinearity between parameters. The number of samples at each stage were as follows: n = 15 (early stage), n = 28 (middle stage), n = 34 (late stage), and n = 62 (reproductive stage).

The corn growth season could be divided into the early (day 38), middle (day 57, 71), late (day 87, 100), and reproductive stages (day 57–100) based on the number of days after emergence. The correlation between CCC and vertical LCC varied between growth stages. In the early growth stage, the highest correlation between LCC and CCC was found at the L6 position (R^2-adj = 0.9, Beta = 0.95). In the middle growth stage, L9 and L16 had the best correlation with CCC (R^2-adj = 0.93). In the late growth stage, the sensitive leaf positions were L9 and L14 (R^2-adj = 0.97). The reproductive stage refers to the entire period from silking to maturity (i.e., the middle and late stages), and in this stage, L11 and L14 were the sensitive leaf positions (R^2-adj = 0.93).

According to the relationship between the chlorophyll content in per unit leaf areas and the chlorophyll content per unit ground area, LAI can be ignored in CCC estimation. Based on the relationships described above for each growth stage, CCC can be estimated directly by leaf spectral reflectance.

3.7. Estimation and Validation of CCC by Leaf Spectral Reflectance

Chlorophyll-related vegetation indices were used to estimate the LCC of sensitive leaf positions at each growth stage based on leaf spectral reflectance. The data from 2019 and 2020 verified that mRER had the best inversion precision for LCC (R^2 = 0.87, Section 3.5), and the average rRMSE of LCC inversion at sensitive leaf positions (such as L14 and L11) was 11.28%. The independent data were sampled at the sixteen-leaf stage (day 51, V16), silking stage (day 64, R1), and filling stage (day 87, R3) in 2019, and these data were used to assess the accuracy of CCC estimation using an MSR model (Figure 6). Separate models were built for the middle, late, and reproductive stages to verify the performance at the three growth stages (Table 5).

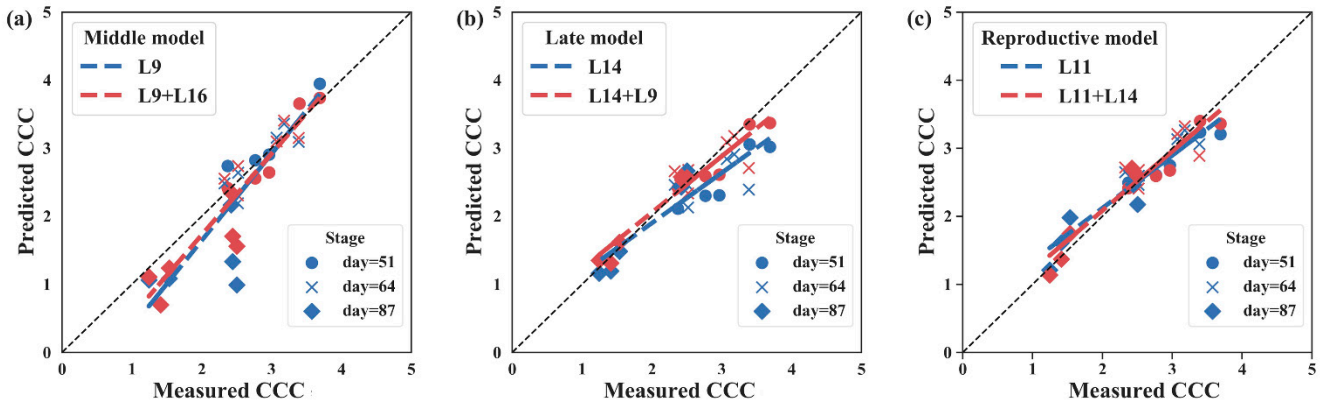

Figure 6. The canopy chlorophyll content (CCC) predicted by the middle model (**a**), late model (**b**), and reproductive model (**c**) compared to measured CCC in 2019. LCC was predicted from mRER, which had the highest accuracy of chlorophyll inversion in this study. The blue dotted line indicates predicted CCC from LCC of one leaf position, and the red line indicates predicted CCC from LCC of two leaf positions. The 2019 dataset included three growth stages: the sixteen-leaf stage (day 51, V16), silking stage (day 64, R1), and filling stage (day 87, R3).

Table 5. Verification of the stepwise regression model in 2019.

Stage	Middle Model		Late Model		Reproductive Model	
	L9	L9 + L16	L14	L14 + L9	L11	L11 + L14
Sixteen-leaf stage (day 51)	7.68%	6.81%	16.60%	7.52%	8.65%	6.95%
Silking stage (day 64)	7.49%	7.26%	16.31%	11.40%	6.96%	9.99%
Filling stage (day 87)	43.95%	30.20%	6.47%	5.46%	13.58%	9.54%
All stages (day 51–87)	20.74%	14.90%	15.35%	9.21%	9.37%	8.97%

Notes: Sample data for the sixteen-leaf stage (day 51, V16), silking stage (day 64, R1), filling stage (day 87, R3), and all stages (days 51–87, n = 18) in 2019 were verified with the three MSR models (middle model, late model, reproductive model). LCC was estimated by mRER (R^2 = 0.87). rRMSE (%) was used to represent error between predicted CCC and measured CCC; smaller rRMSE values correspond to higher model accuracy.

The validation results (Table 5) showed that MSR models could accurately estimate CCC from leaf spectral reflectance. The middle stage model had good estimation accuracy in the V16 and silking stages (with rRMSE values of 6.81% and 7.26%, respectively) but poor estimation at the filling stage (rRMSE = 30.2%). The late model had high precision for CCC estimation at the filling stage (rRMSE = 6.47%), but low precision at the V16 and silking stages (rRMSE values of 16.6% and 16.31%, respectively). The reproductive stage model was constructed by integrating data from silking through maturation stages in 2020, and this model showed high accuracy for CCC estimation throughout all three growth stages in 2019 (rRMSE ranged from 6.95–9.99%).

Compared with establishing relationships between CCC and LCC at a single leaf position, estimating CCC using LCC values from two sensitive leaf positions showed higher accuracy and robustness (Table 5). Thus, CCC (g/m^2) can be accurately estimated from LCC ($\mu g/cm^2$) at the L11 and L14 positions based on leaf spectral reflectance (rRMSE = 8.97%) at the reproductive stage.

4. Discussion

Remote sensing of chlorophyll is a fundamental component of the quantitative remote sensing of crops. Many studies have addressed the vertical distribution of chlorophyll in the canopy because understanding canopy architecture is important for crop growth management and monitoring [5,27]. Solar radiation interception of the canopy structure and nitrogen transference have been identified as the main contributors to vertical heterogeneity of the chlorophyll content in the canopy [5,9,10]. In the present study, vertical distribution of the leaf chlorophyll content (LCC) in the canopy and changes in the correlation between LCC and leaf spectral reflectance were explored. The vertical profile of LCC showed asymmetric distribution, with higher values in the upper–middle layer than in the top or bottom layers [7,8]. In the vegetative stage, the highest values were found in the lower–middle layer (Figure 2). The bottom layers of the canopy were significantly affected by nitrogen supply [14,31]; it appears that a sufficient nitrogen supply can ensure that leaves continue to synthesize chlorophyll and remain vital as the plant matures.

We created a variety of canopy architecture types by applying different amounts of nitrogen fertilizer (Figure 2), as has been done in previous studies [7,8]. The green band at 531–567 nm and the red-edge (RE) band at 712–731 nm were sensitive to chlorophyll (Figure 3) [3]. Vegetation index (VI) models based on leaf spectral reflectance could effectively achieve LCC inversion. mRER was the VI with the best LCC modeling performance in this study (R^2 = 0.87). Red edge (RE) and near-infrared (NIR) were the necessary bands to measure to build the VI–chlorophyll model (Table 3) [3,27]. The RE waveband had a moderate correlation with chlorophyll (r = −0.77), but the correlation with NIR was not significant. Previous studies showed that there are specific absorption bands in the NIR waveband that are associated with nitrogen and proteins, and these are related to the vertical distribution of nitrogen in the canopy [55].

Leaf spectral reflectance has been widely used in previous research for remote sensing, and it has been shown that leaf reflectance varies throughout the canopy [56,57]. However, there are few conclusions about whether there is a unified chlorophyll–spectral relationship

for different leaf positions in the canopy. To determine the relationship between LCC and leaf spectral reflectance, a VI–LCC model was established here and verified under several spatio-temporal conditions. The results showed that there was a great deal of variability in the relationship between LCC and leaf spectra at different positions in the canopy, and a single VI–chlorophyll model was limited in its capacity to predict LCC (Figure 5). However, the inversion effect of the chlorophyll model was consistent within each growth stage. Other researchers have published similar results in using SPAD to monitor leaf chlorophyll and the nitrogen content [58–61]. Here, the VI model could invert LCC well in the middle growth stage (day 57–71), and L13–L15 had the best inversion accuracy (rRMSE ≈ 6.6%). However, VI and LCC had weak positive correlations in the tender upper leaves at the vegetative growth stage (day 38, L10–L14, rRMSE ≈ 70.3%) and in the aged leaves in the upper-lower positions at the late reproductive growth stage (day 100, L10–L12 and L16–L18, rRMSE ≈ 61.5%). In the early growth stage, differences in leaf spectra between leaf positions were concentrated in the RE and NIR waveband regions, indicating that the leaf microstructure differed by leaf position. In contrast, in the late stage, differences were concentrated in the visible region, indicating a difference in the chlorophyll content between leaf positions [14,37]. However, there were six VI models for chlorophyll inversion that performed with consistent accuracy, showing that the variation may be caused by changes in leaf structure or chlorophyll spectral properties rather than by VI sensitivity [13,62].

Previous studies reported that crops respond to deficiency or stress by altering the chlorophyll content at different vertical leaf positions to maintain photosynthetic efficiency [56,63,64]. The chlorophyll content in the collar leaf at the vegetation stage and in the ear leaf at the reproductive stage is often used to evaluate the canopy chlorophyll status [30,32], and other research suggested that bottom leaf positions were more suitable as indicators of canopy chlorophyll diagnosis [65,66]. In the present study, data collected in 2019 and 2020 demonstrated a strong correlation between CCC and LCC at various growth stages. Based on a multiple stepwise regression (MSR) model, CCC could be accurately estimated from the chlorophyll content at multiple leaf positions. L6 in the vegetative stage (R^2-adj = 0.9) and L11 + L14 in the reproductive stage (R^2-adj = 0.93) were used as the sensitive leaf positions for CCC estimation. Based on the close correlation between leaf spectral reflectance and the chlorophyll content per unit of leaf area (LCC, μg/cm^2), the MSR model of CCC estimation was established using a VI model; mRER represents LCC, and the high accuracy was verified at different growth stages (rRMSE = 8.97%). Due to the strong correlation between LCC at vertical leaf positions [18], CCC estimated using LCC from two sensitive leaf positions was a better choice to avoid multilinearity and improve model precision.

The leaves were usually considered to be uniform objects in previous studies, which means the relationship between LCC and leaf spectral reflectance is consistent in the same plant species [33,67,68]. Other studies proposed that the leaf thickness, water content, and leaf structure would lead to inconsistencies between LCC and spectral reflectance [22,69,70]. A common viewpoint is that there are strong correlations between LCC and spectral characteristics in the middle leaf position of a canopy, with a weak relationship in the upper and lower positions of the canopy [56]. In the present study, a more elaborate division of growth stages and vertical distribution was conducted, illustrating the variability of the correlation between LCC and leaf spectral reflectance under various spatial-temporal conditions. The mismatch between the LCC and spectral would be masked by the soil background and canopy architecture that make chlorophyll remote sensing at a canopy level more complicated with a lack of robustness.

Canopy spectral reflectance (measured using a UAV or satellite) is an efficient and non-destructive chlorophyll remote sensing method. However, ignoring the significant vertical gradient of chlorophyll and treating the canopy as a uniform plane field would limit robustness and decrease the practical value of canopy remote sensing [7,71]. On the one hand, previous studies proposed that chlorophyll deficiency is mainly exhibited in the lower positions of the canopy rather than in the upper leaves [14,65]. On the other hand,

canopy spectral reflectance is mainly contributed by the upper–middle leaves, and few studies explored CCC estimation from part of LCC in the canopy [72,73]. In this study, a CCC estimation model based on the LCC vertical distribution was proposed, which avoids the influence of LAI and biomass. The LCC of lower leaves (L6) at the vegetative stage and upper–mid leaves (L11, L14) at the reproductive stage was sensitive to CCC changes. This result provides theoretical support and reference sensitive leaf positions for canopy chlorophyll remote sensing, considering the non-uniform vertical distribution [29,34,74].

Some limitations of this study should be mentioned. The vegetative stage is an important period in which crops accumulate material, and due to limitations on the number of sampling time points, the vertical distribution of LCC and verification of sensitive leaf positions in this stage have not been fully demonstrated. Additionally, only the maize variety JNK728 was studied, preventing comparison among different varieties. The factors leading to the observed inconsistent relationship between LCC and VI at the early and late growth stages need further study. Additional time points and maize varieties will be studied in future research to address these issues.

5. Conclusions

Five nitrogen application levels were used to construct diverse maize canopy architectures and reveal the vertical heterogeneity of the leaf chlorophyll content (LCC) and leaf spectral reflectance characteristics in the maize canopy. A multiple stepwise regression (MSR) model was built to accurately monitor the canopy chlorophyll content (CCC) based on the vertical distribution of LCC within the canopy; LCC showed an asymmetric vertical distribution, tending to be lower in the bottom layer, increasing in the middle layer, then decreasing in the upper layer. Nitrogen treatments significantly changed LCC, and the vertical profile of LCC distribution remained similar between treatments. Leaf spectral reflectance characteristics under variable spatio–temporal conditions were analyzed. The green band (531–567 nm) and the red-edge band (712–731 nm) were the sensitive wavebands for monitoring LCC. Six classical VIs were used to construct VI–chlorophyll models, the best of which was the model built with modified red-edge ratio (mRER, R^2 = 0.87). The VI model could accurately predict LCC at the middle growth stage (rRMSE = 10.9%), but the correlation between VI and LCC changed in the upper and lower leaf layers during the early vegetative and mature stages (rRMSE ranged from 36% to 87%). Through a combination of the inversion accuracy results and multiple stepwise regression, the leaves at positions L6 in the vegetative stage and L11 and L14 in the reproductive stage (L12 is the ear leaf) were found to be the most sensitive in CCC estimation. In this way, a VI–LCC–CCC model was constructed based on leaf spectral reflectance to estimate the canopy chlorophyll status. The model was evaluated using data from field experiments in 2019 and 2020 and was found to be robust and accurate (rRMSE = 8.97%).

Author Contributions: Conceptualization, H.Y., K.W., B.M. and S.L.; methodology, H.Y., R.X., C.N. and B.M.; investigation, H.Y., B.X., X.L., J.X. (Jiangfeng Xin), P.H. and J.X. (Jun Xue); writing—original draft preparation, H.Y. and B.M. All authors have read and agreed to the published version of the manuscript.

Funding: This research was supported by the National Key Research and Development Program of China (2016YFD0300605), China Agriculture Research System of MOF and MARA, and the Agricultural Science and Technology Innovation Program (CAAS-ZDRW202004).

Data Availability Statement: Not applicable.

Acknowledgments: We gratefully thank the Xinxiang Experimental Station for the experiment support.

Conflicts of Interest: The authors declare no conflict of interest.

Appendix A

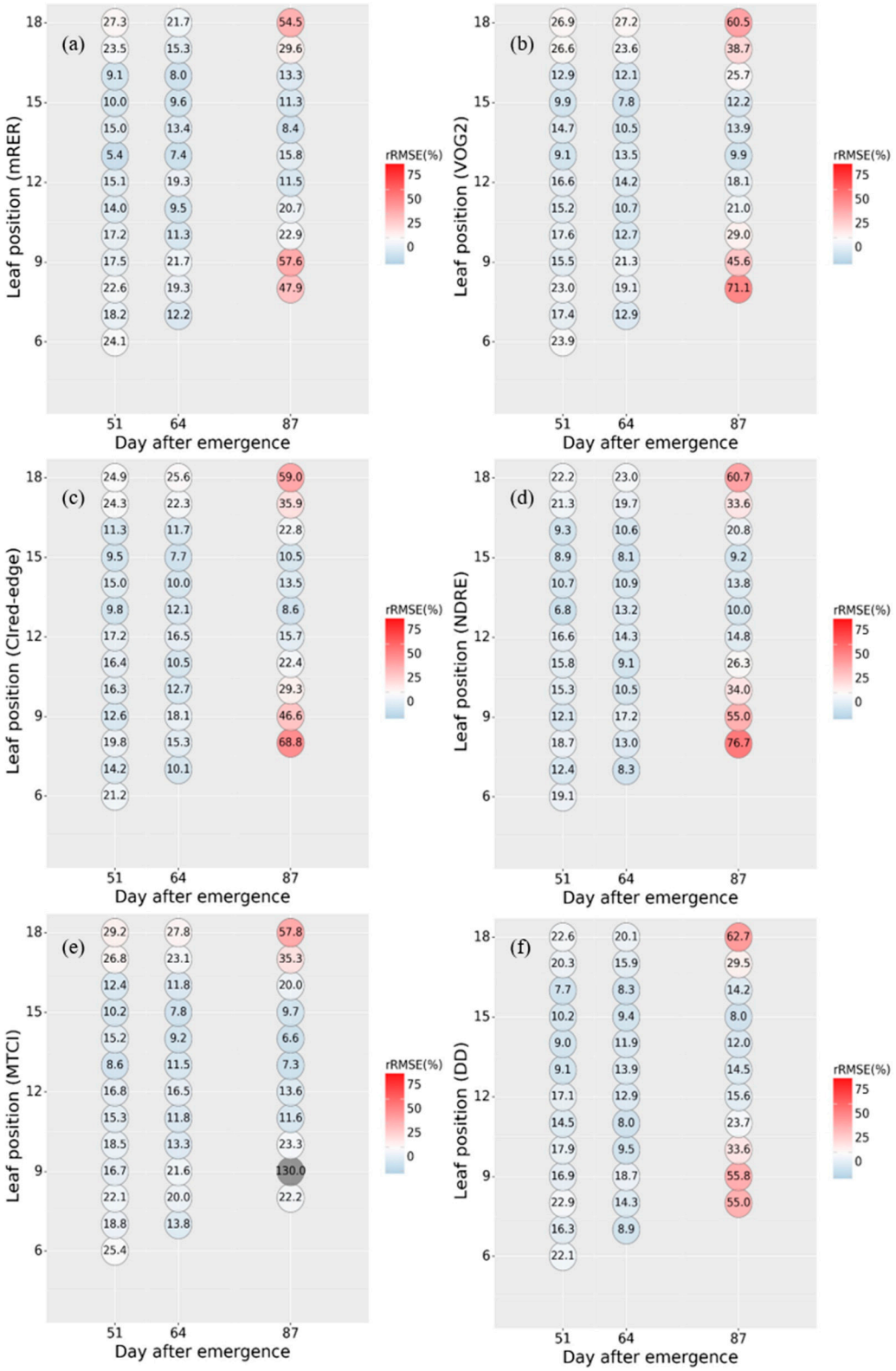

Figure A1. rRMSE (%) of the six LCC–VI models (2019): (**a**) mRER, (**b**) VOG2, (**c**) CIred-edge, (**d**) NDRE, (**e**) MTCI, and (**f**) DD. rRMSE was used to evaluate the consistency of model inversion.

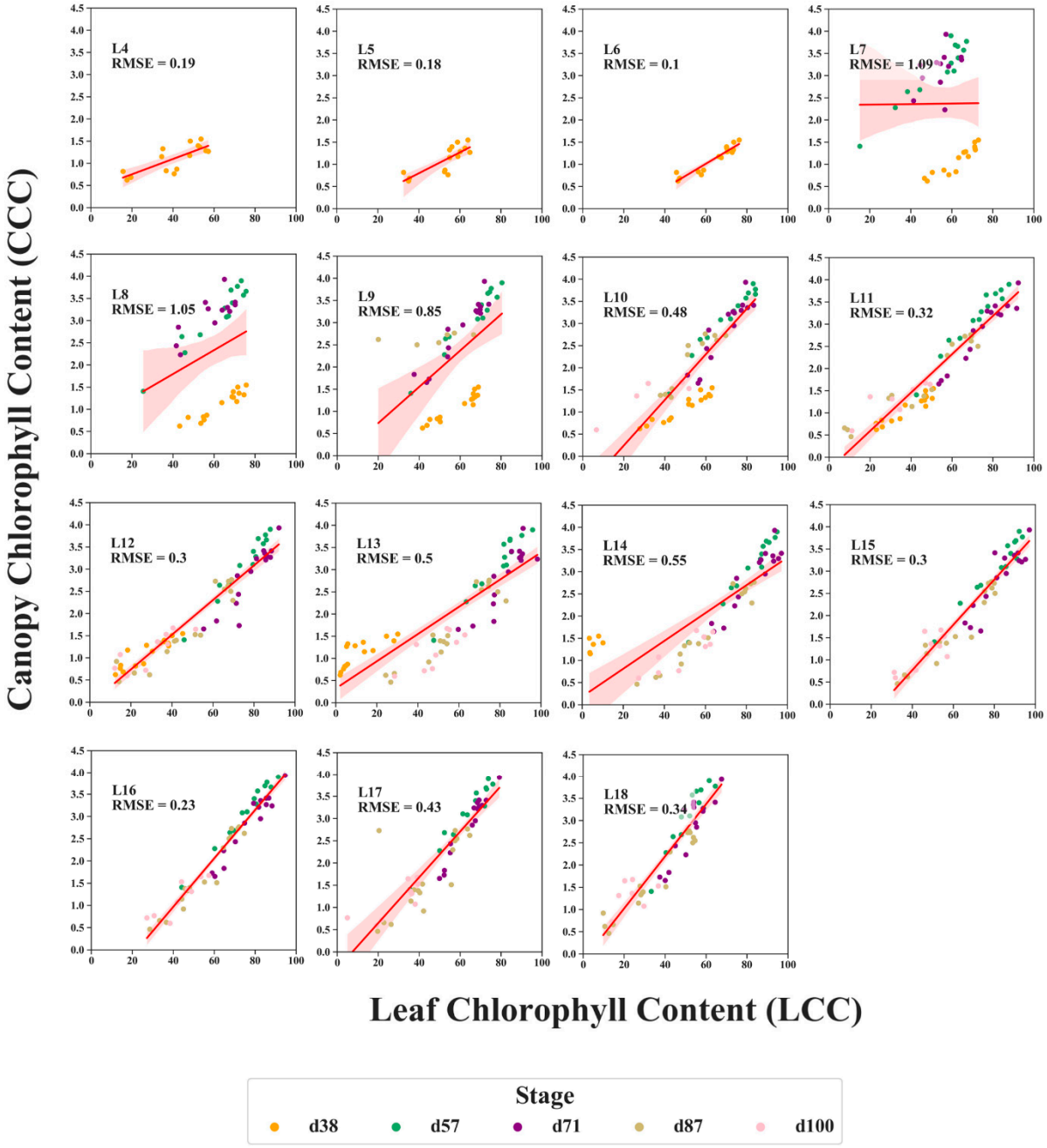

Figure A2. Relationships between the chlorophyll content in the leaf (LCC) and chlorophyll content in the canopy (CCC) at each leaf position and growth stage. Leaf position corresponds to the order of emergence from the bottom to the top of the canopy (L4–L18).

References

1. Xue, L.H.; Cao, W.X.; Yang, L.Z. Predicting Grain Yield and Protein Content in Winter Wheat at Different N Supply Levels Using Canopy Reflectance Spectra. *Pedosphere* **2007**, *17*, 646–653. [CrossRef]
2. Prey, L.; Hu, Y.; Schmidhalter, U. High-Throughput Field Phenotyping Traits of Grain Yield Formation and Nitrogen Use Efficiency: Optimizing the Selection of Vegetation Indices and Growth Stages. *Front. Plant Sci.* **2020**, *10*, 1672. [CrossRef]
3. Daughtry, C.S.T.; Walthall, C.L.; Kim, M.S.; de Colstoun, E.B.; McMurtrey, J.E. Estimating Corn Leaf Chlorophyll Concentration from Leaf and Canopy Reflectance. *Remote Sens. Environ.* **2000**, *74*, 229–239. [CrossRef]
4. Li, D.; Chen, J.M.; Zhang, X.; Yan, Y.; Zhu, J.; Zheng, H.; Zhou, K.; Yao, X.; Tian, Y.; Zhu, Y.; et al. Improved estimation of leaf chlorophyll content of row crops from canopy reflectance spectra through minimizing canopy structural effects and optimizing off-noon observation time. *Remote Sens. Environ.* **2020**, *248*, 111985. [CrossRef]

5. Li, H.; Zhao, C.; Huang, W.; Yang, G. Non-uniform vertical nitrogen distribution within plant canopy and its estimation by remote sensing: A review. *Field Crops Res.* **2013**, *142*, 75–84. [CrossRef]
6. Wang, Q.; Li, P. Canopy vertical heterogeneity plays a critical role in reflectance simulation. *Agric. For. Meteorol.* **2013**, *169*, 111–121. [CrossRef]
7. Winterhalter, L.; Mistele, B.; Schmidhalter, U. Assessing the vertical footprint of reflectance measurements to characterize nitrogen uptake and biomass distribution in maize canopies. *Field Crops Res.* **2012**, *129*, 14–20. [CrossRef]
8. Ciganda, V.; Gitelson, A.; Schepers, J. Vertical Profile and Temporal Variation of Chlorophyll in Maize Canopy: Quantitative "Crop Vigor" Indicator by Means of Reflectance-Based Techniques. *Agron. J.* **2008**, *100*, 1409–1417. [CrossRef]
9. Hikosaka, K.; Anten, N.P.; Borjigidai, A.; Kamiyama, C.; Sakai, H.; Hasegawa, T.; Oikawa, S.; Iio, A.; Watanabe, M.; Koike, T.; et al. A meta-analysis of leaf nitrogen distribution within plant canopies. *Ann. Bot.* **2016**, *118*, 239–247. [CrossRef]
10. Hirose, T.; Werger, M. Maximizing Daily canopy photosynthesis with respect to the leaf nitrogen allocation pattern in the canopy. *Oecologia* **1987**, *72*, 520–526. [CrossRef]
11. Zhao, C.; Hang, W.; Wang, J.; Liu, L.; Song, X.; Ma, Z.; Li, C. Extracting winter wheat chlorophyll concentration vertical distribution based on bidirectional canopy reflected spectrum. *Trans. Chin. Soc. Agric. Eng.* **2006**, *22*, 104–109. (In Chinese) [CrossRef]
12. Gitelson, A.; Gritz, Y.; Merzlyak, M. Relationships between leaf chlorophyll content and spectral reflectance and algorithms for non-destructive chlorophyll assessment in higher plant leaves. *J. Plant Physiol.* **2003**, *160*, 271–282. [CrossRef]
13. Sims, D.; Gamon, J. Relationships between Leaf Pigment Content and Spectral Reflectance across a Wide Range of Species, Leaf Structures and Developmental Stages. *Remote Sens. Environ.* **2002**, *81*, 337–354. [CrossRef]
14. Lu, Y.-L.; Bai, Y.-L.; Ma, D.-L.; Wang, L.; Yang, L.-P. Nitrogen Vertical Distribution and Status Estimation Using Spectral Data in Maize. *Commun. Soil Sci. Plant Anal.* **2018**, *49*, 526–536. [CrossRef]
15. Gitelson, A.; Merzlyak, M. Spectral Reflectance Changes Associated with Autumn Senescence of *Aesculus hippocastanum* L. and *Acer platanoides* L. Leaves. Spectral Features and Relation to Chlorophyll Estimation. *J. Plant Physiol.* **1994**, *143*, 286–292. [CrossRef]
16. Dash, J.; Curran, P. The MERIS terrestrial chlorophyll index. *Int. J. Remote Sens.* **2004**, *25*, 5003–5013. [CrossRef]
17. Vogelmann, J.E.; Rock, B.N.; Moss, D.M. Red edge spectral measurements from sugar maple leaves. *Int. J. Remote Sens.* **1993**, *14*, 1563–1575. [CrossRef]
18. Ciganda, V.; Gitelson, A.; Schepers, J.S. How deep does a remote sensor sense? Expression of chlorophyll content in a maize canopy. *Remote Sens. Environ.* **2012**, *126*, 240–247. [CrossRef]
19. Lee, Y.; Yang, C.-M.; Chang, K.W.; Shen, Y. Effects of nitrogen status on leaf anatomy, chlorophyll content and canopy reflectance of paddy rice. *Bot. Stud.* **2011**, *52*, 295–303.
20. Wan, L.; Zhou, W.; He, Y.; Wanger, T.C.; Cen, H. Combining transfer learning and hyperspectral reflectance analysis to assess leaf nitrogen concentration across different plant species datasets. *Remote Sens. Environ.* **2022**, *269*, 112826. [CrossRef]
21. Li, L.T.; Jakli, B.; Lu, P.P.; Ren, T.; Ming, J.; Liu, S.S.; Wang, S.Q.; Lu, J.W. Assessing leaf nitrogen concentration of winter oilseed rape with canopy hyperspectral technique considering a non-uniform vertical nitrogen distribution. *Ind. Crops Prod.* **2018**, *116*, 1–14. [CrossRef]
22. Wang, Z.H.; Skidmore, A.K.; Darvishzadeh, R.; Heiden, U.; Heurich, M.; Wang, T.J. Leaf Nitrogen Content Indirectly Estimated by Leaf Traits Derived From the PROSPECT Model. *IEEE J. Sel. Top. Appl. Earth Obs. Remote Sens.* **2015**, *8*, 3172–3182. [CrossRef]
23. Jacquemoud, S.; Verhoef, W.; Baret, F.; Bacour, C.; Zarco-Tejada, P.J.; Asner, G.P.; François, C.; Ustin, S.L. PROSPECT+SAIL models: A review of use for vegetation characterization. *Remote Sens. Environ.* **2009**, *113*, S56–S66. [CrossRef]
24. Chakhvashvili, E.; Siegmann, B.; Muller, O.; Verrelst, J.; Bendig, J.; Kraska, T.; Rascher, U. Retrieval of Crop Variables from Proximal Multispectral UAV Image Data Using PROSAIL in Maize Canopy. *Remote Sens.* **2022**, *14*, 1247. [CrossRef]
25. Zhang, D.; Wang, X.; Ma, W.; Zhao, C. Research Vertical Distribution of Chlorophyll Content of Wheat Leaves Using Imaging Hyperspectra. *Intell. Autom. Soft Comput.* **2012**, *18*, 1111–1120. [CrossRef]
26. Yang, H.; Li, J.; Yang, J.; Wang, H.; Zou, J.; He, J. Effects of nitrogen application rate and leaf age on the distribution pattern of leaf SPAD readings in the rice canopy. *PLoS ONE* **2014**, *9*, e88421. [CrossRef]
27. Wu, B.; Ye, H.; Huang, W.; Wang, H.; Luo, P.; Ren, Y.; Kong, W. Monitoring the Vertical Distribution of Maize Canopy Chlorophyll Content Based on Multi-Angular Spectral Data. *Remote Sens.* **2021**, *13*, 987. [CrossRef]
28. Huang, W.J.; Yang, Q.Y.; Peng, D.L.; Huang, L.S.; Zhang, D.Y.; Yang, G.J. Nitrogen vertical distribution by canopy reflectance spectrum in winter wheat. In *IOP Conference Series: Earth and Environmental Science*; IOP Publishing: Bristol, UK, 2014; Volume 17. [CrossRef]
29. Wu, B.; Huang, W.; Ye, H.; Luo, P.; Ren, Y.; Kong, W. Using Multi-Angular Hyperspectral Data to Estimate the Vertical Distribution of Leaf Chlorophyll Content in Wheat. *Remote Sens.* **2021**, *13*, 1501. [CrossRef]
30. Ciganda, V.; Gitelson, A.; Schepers, J. Non-destructive determination of maize leaf and canopy chlorophyll content. *J. Plant Physiol.* **2009**, *166*, 157–167. [CrossRef]
31. Klem, K.; Rajsnerová, P.; Novotná, K.; Mìša, P.; Křen, J. Changes in Vertical Distribution of Spectral Reflectance within Spring Barley Canopy as an Indicator of Nitrogen Nutrition, Canopy Structure and Yield Parameters. *Agriculture* **2014**, *60*, 50–59. [CrossRef]
32. Li, Z.; Zhang, Y.; Liu, H.; Zhang, F. Application of chlorophyll meter on N nutritional diagnosis for summer corn. *Plant Nutr. Fertitizer Sci.* **2005**, *11*, 764–768.

33. Gitelson, A.A.; Vina, A.; Ciganda, V.; Rundquist, D.C.; Arkebauer, T.J. Remote estimation of canopy chlorophyll content in crops. *Geophys. Res. Lett.* **2005**, *32*, L08403. [CrossRef]
34. Duan, D.D.; Zhao, C.J.; Li, Z.H.; Yang, G.J.; Zhao, Y.; Qiao, X.J.; Zhang, Y.H.; Zhang, L.X.; Yang, W.D. Estimating total leaf nitrogen concentration in winter wheat by canopy hyperspectral data and nitrogen vertical distribution. *J. Integr. Agric.* **2019**, *18*, 1562–1570. [CrossRef]
35. Ye, H.; Huang, W.; Huang, S.; Wu, B.; Dong, Y.; Cui, B. Remote Estimation of Nitrogen Vertical Distribution by Consideration of Maize Geometry Characteristics. *Remote Sens.* **2018**, *10*, 1995. [CrossRef]
36. Li, D.; Guo, Y.; Yun, H.; Zhang, M.; Gong, X.; Fang, M. Dtermined Methods of Chlorophyll from Maize. *Chin. Agric. Sci. Bull.* **2005**, *21*, 153. (In Chinese)
37. Wen, P.F.; Shi, Z.J.; Li, A.; Ning, F.; Zhang, Y.H.; Wang, R.; Li, J. Estimation of the vertically integrated leaf nitrogen content in maize using canopy hyperspectral red edge parameters. *Precis. Agric.* **2021**, *22*, 984–1005. [CrossRef]
38. Cheng, M.; Jiao, X.; Liu, Y.; Shao, M.; Yu, X.; Bai, Y.; Wang, Z.; Wang, S.; Tuohuti, N.; Liu, S.; et al. Estimation of soil moisture content under high maize canopy coverage from UAV multimodal data and machine learning. *Agric. Water Manag.* **2022**, *264*, 107530. [CrossRef]
39. Jordan, C.F. Derivation of Leaf-Area Index from Quality of Light on the Forest Floor. *Ecology* **1969**, *50*, 663–666. [CrossRef]
40. Rouse, J.; Haas, R.; Schell, J.; Deering, D.; Harlan, J. *Monitoring the Vernal Advancement and Retrogradation (Green Wave Effect) of Natural Vegetation*; NASA/GSFC Type III, Final Report; NASA: Greenbelt, MD, USA, 1974.
41. Gitelson, A.; Merzlyak, M. Remote sensing of chlorophyll concentration in higher plant leaves. *Adv. Space Res.* **1998**, *22*, 689–692. [CrossRef]
42. Metternicht, G. Vegetation indices derived from high-resolution airborne videography for precision crop management. *Int. J. Remote Sens.* **2003**, *24*, 2855–2877. [CrossRef]
43. Fitzgerald, G.; Rodriguez, D.; O'Leary, G. Measuring and predicting canopy nitrogen nutrition in wheat using a spectral index—The canopy chlorophyll content index (CCCI). *Field Crops Res.* **2010**, *116*, 318–324. [CrossRef]
44. Haboudane, D.; Miller, J.; Tremblay, N.; Zarco-Tejada, P.; Dextraze, L. Integrated narrow-band vegetation indices for prediction of crop chlorophyll content for application to precision agriculture. *Remote Sens. Environ.* **2002**, *81*, 416–426. [CrossRef]
45. Strachan, I.; Pattey, E.; Boisvert, J. Impact of nitrogen and environmental conditions on corn as detected by hyperspectral reflectance. *Remote Sens. Environ.* **2002**, *80*, 213–224. [CrossRef]
46. le Maire, G.; Francois, C.; Dufrêne, E. Towards universal broad leaf chlorophyll indices using PROSPECT simulated database and hyperspectral reflectance measurements. *Remote Sens. Environ.* **2004**, *89*, 1–28. [CrossRef]
47. Broge, N.; Leblanc, E. Comparing prediction power and stability of broadband and hyperspectral vegetation indices for estimation of green leaf area index and canopy chlorophyll density. *Remote Sens. Environ.* **2001**, *76*, 156–172. [CrossRef]
48. Jay, S.; Gorretta, N.; Morel, J.; Maupas, F.; Bendoula, R.; Rabatel, G.; Dutartre, D.; Comar, A.; Frederic, B. Estimating leaf chlorophyll content in sugar beet canopies using millimeter- to centimeter-scale reflectance imagery. *Remote Sens. Environ.* **2017**, *198*, 173–186. [CrossRef]
49. Chen, P.; Haboudane, D.; Tremblay, N.; Wang, J.; Baoguo, L. New spectral indicator assessing the efficiency of crop nitrogen treatment in corn and wheat. *Remote Sens. Environ.* **2010**, *114*, 1987–1997. [CrossRef]
50. Feng, W.; Guo, B.-B.; Zhang, H.-Y.; He, L.; Zhang, Y.-S.; Wang, Y.-H.; Zhu, Y.-J.; Guo, T.-C. Remote estimation of above ground nitrogen uptake during vegetative growth in winter wheat using hyperspectral red-edge ratio data. *Field Crops Res.* **2015**, *180*, 197–206. [CrossRef]
51. Peng, Y.; Nguy-Robertson, A.; Arkebauer, T.; Gitelson, A. Assessment of Canopy Chlorophyll Content Retrieval in Maize and Soybean: Implications of Hysteresis on the Development of Generic Algorithms. *Remote Sens.* **2017**, *9*, 226. [CrossRef]
52. Huang, Z.; Turner, B.J.; Dury, S.J.; Wallis, I.R.; Foley, W.J. Estimating foliage nitrogen concentration from HYMAP data using continuum removal analysis. *Remote Sens. Environ.* **2004**, *93*, 18–29. [CrossRef]
53. Feng, A.; Zhou, J.; Vories, E.D.; Sudduth, K.A.; Zhang, M. Yield estimation in cotton using UAV-based multi-sensor imagery. *Biosyst. Eng.* **2020**, *193*, 101–114. [CrossRef]
54. Zhang, H.Y.; Ren, X.X.; Yi, Z.; Wu, Y.P.; Li, H.; Ya-Rong, H.; Wei, F.; Wang, C.Y. Remotely assessing photosynthetic nitrogen use efficiency with in situ hyperspectral remote sensing in winter wheat. *Eur. J. Agron.* **2018**, *101*, 90–100. [CrossRef]
55. Berger, K.; Verrelst, J.; Féret, J.-B.; Wang, Z.; Wocher, M.; Strathmann, M.; Danner, M.; Mauser, W.; Hank, T. Crop nitrogen monitoring: Recent progress and principal developments in the context of imaging spectroscopy missions. *Remote Sens. Environ.* **2020**, *242*, 111758. [CrossRef]
56. Zhang, Y.-J.; Wang, L.; Bai, Y.-L. Nitrogen Nutrition Diagnostic Based on Hyperspectral Analysis about Different Layers Leaves in Maize. *Spectrosc. Spectr. Anal.* **2019**, *39*, 2829. (In Chinese)
57. Xu, X.; Li, Z.; Yang, X.; Yang, G.; Teng, C.; Zhu, H.; Liu, S. Predicting leaf chlorophyll content and its nonuniform vertical distribution of summer maize by using a radiation transfer model. *J. Appl. Remote Sens.* **2019**, *13*, 034505. [CrossRef]
58. Zhang, Y.-J.; Wang, L.; Bai, Y.; Lu, Y.-L.; Zhang, J.-J.; Ge, L. Relationship of physiological and biochemical indicators with SPAD values in maize leaves at different layers. *J. Plant Nutr. Fertil.* **2020**, *26*, 61–73. (In Chinese)
59. Zhao, B.; Tahir, A.; Liu, Z.; Zhang, J.; Xiao, J.; Liu, Z.; Qin, A.; Ning, D.; Yang, Q.; Zhang, Y. Simple Assessment of Nitrogen Nutrition Index in Summer Maize by Using Chlorophyll Meter Readings. *Front. Plant Ence* **2018**, *9*, 11. [CrossRef]

60. Dang, R.J.; Li, S.-Q.; Mu, X.-H.; Li, S.-X. Effect of nitrogen on vertical distribution of canopy nitrogen and chlorophyll relative value (SPAD value) of summer maize in sub-humid areas. *Chin. J. Eco-Agric.* **2009**, *17*, 54–59. [CrossRef]
61. Peng, S.; Laza, M.; Garcia, F.V.; Cassman, K.G. Chlorophyll meter estimates leaf area-based nitrogen concentration of rice. *Commun. Soil Sci. Plant Anal.* **1995**, *26*, 927–935. [CrossRef]
62. Féret, J.-B.; Francois, C.; Asner, G.; Gitelson, A.; Martin, R.; Bidel, L.; Ustin, S.; le Maire, G.; Jacquemoud, S. PROSPECT-4 and 5: Advances in the leaf optical properties model separating photosynthetic pigments. *Remote Sens. Environ.* **2008**, *112*, 3030–3043. [CrossRef]
63. Li, Z.; Jin, X.; Yang, G.; Drummond, J.; Yang, H.; Clark, B.; Li, Z.; Zhao, C. Remote Sensing of Leaf and Canopy Nitrogen Status in Winter Wheat (*Triticum aestivum* L.) Based on N-PROSAIL Model. *Remote Sens.* **2018**, *10*, 1463. [CrossRef]
64. Li, L.; Sheng, K.; Yin, H.; Guo, Y.; Wang, D.; Wang, Y. Selecting the sensitive position of maize leaves for nitrogen status diagnosis of summer maize by considering vertical nitrogen distribution in plant. *Trans. Chin. Soc. Agric. Eng.* **2020**, *36*, 64–73. [CrossRef]
65. Huang, W.; Yang, Q.; Pu, R.; Yang, S. Estimation of Nitrogen Vertical Distribution by Bi-Directional Canopy Reflectance in Winter Wheat. *Sensors* **2014**, *14*, 20347–20359. [CrossRef]
66. Wang, Z.; Wang, J.; Zhao, C.; Zhao, M.; Huang, W.; Wang, C. Vertical Distribution of Nitrogen in Different Layers of Leaf and Stem and Their Relationship with Grain Quality of Winter Wheat. *J. Plant Nutr.* **2005**, *28*, 73–91. [CrossRef]
67. Wan, L.; Zhang, J.; Xu, Y.; Huang, Y.; Zhou, W.; Jiang, L.; He, Y.; Cen, H. PROSDM: Applicability of PROSPECT model coupled with spectral derivatives and similarity metrics to retrieve leaf biochemical traits from bidirectional reflectance. *Remote Sens. Environ.* **2021**, *267*, 112761. [CrossRef]
68. Wang, H.F.; Huo, Z.G.; Zhou, G.S.; Liao, Q.H.; Feng, H.K.; Wu, L. Estimating leaf SPAD values of freeze-damaged winter wheat using continuous wavelet analysis. *Plant Physiol Biochem.* **2016**, *98*, 39–45. [CrossRef]
69. Liu, L.; Song, B.; Zhang, S.; Liu, X. A Novel Principal Component Analysis Method for the Reconstruction of Leaf Reflectance Spectra and Retrieval of Leaf Biochemical Contents. *Remote Sens.* **2017**, *9*, 1113. [CrossRef]
70. Jacquemoud, S.; Ustin, S.L.; Verdebout, J.; Schmuck, G.; Andreoli, G.; Hosgood, B. Estimating leaf biochemistry using the PROSPECT leaf optical properties model. *Remote Sens. Environ.* **1996**, *56*, 194–202. [CrossRef]
71. Li, H.; Zhao, C.; Yang, G.; Feng, H. Variations in crop variables within wheat canopies and responses of canopy spectral characteristics and derived vegetation indices to different vertical leaf layers and spikes. *Remote Sens. Environ.* **2015**, *169*, 358–374. [CrossRef]
72. Xiao, C.H.; Li, S.K.; Wang, K.R.; Lu, Y.L.; Bai, J.H.; Xie, R.Z.; Gao, S.J.; Li, X.J.; Tan, H.Z. The Response of Canopy Direction Reflectance Spectrum for the Wheat Vertical Leaf Distributing. *Sens. Lett.* **2009**, *9*, 77–85.
73. Liu, S.; Peng, Y.; Du, W.; Le, Y.; Li, L. Remote Estimation of Leaf and Canopy Water Content in Winter Wheat with Different Vertical Distribution of Water-Related Properties. *Remote Sens.* **2015**, *7*, 4626–4650. [CrossRef]
74. Luo, J.; Ma, R.; Feng, H.; Li, X. Estimating the Total Nitrogen Concentration of Reed Canopy with Hyperspectral Measurements Considering a Non-Uniform Vertical Nitrogen Distribution. *Remote Sens.* **2016**, *8*, 789. [CrossRef]